INTERNATIONAL JOURNAL OF CIRCUIT THEORY AND APPLICATIONS
Int. J. Circ. Theor. Appl. 2004; **32**:471–486
Published online in Wiley InterScience (www.interscience.wiley.com). DOI: 10.1002/cta.279

A reduction technique of large-scale RCG interconnects in the complex frequency domain

Y. Yamagami[1], Y. Tanji[2], A. Hattori[1], Y. Nishio[1] and A. Ushida[1,*,†]

[1]*Department of Electrical and Electronic Engineering, Tokushima University, Tokushima 770-8506, Japan*
[2]*Faculty of Engineering, Kagawa University, 761-0396, Japan*

SUMMARY

High-speed digital LSI chips usually consist of many sub-circuits coupled with multi-conductor interconnects embedded in the substrate. They sometimes cause serious problems of the fault switching operations due to the time-delays, crosstalks, reflections, etc. In order to solve these problems, it is very important to develop a user-friendly simulator for the analysis of LSIs coupled with interconnects. In this paper, we consider a large-scale gate-array circuit coupled with multi-conductor RCG interconnects. At first, we propose a new method for calculating the dominant poles of the impedance matrix, which give the large effects to the transient response. The corresponding residues are estimated by the least squares method. Using these poles and residues, the input–output relation of each interconnect can be described by the partial fractions. After then, the interconnect is replaced by the equivalent circuit realizing the partial fractions. In this way, we can easily develop a user-friendly simulator familiar with SPICE. We found from many examples that the good results can be obtained using only few dominant poles around the origin. Furthermore, the reduction ratio of our method is very large especially for large scale interconnects. Copyright © 2004 John Wiley & Sons, Ltd.

KEY WORDS: IC interconnects; exact poles and residues; reduction algorithm; complex frequency domain; SPICE simulator; asymptotic equivalent circuit; passivity

1. INTRODUCTION

The analysis and design of high-speed LSI chips are becoming more and more important, because the LSI chips coupled with interconnects embedded in the substrate sometimes cause the fault switching operations due to the signal delays, crosstalks, reflections, etc [1–9]. The Elmore resistance–capacitance (RC) delay metric is popular due to its simple closed-form expression, computation speed and fidelity with respect to the simulation [4]. The closed-form combining the delay and crosstalk is firstly shown in Reference [5]. The improved techniques [6–9] are proposed later for improving the accuracy and the practical applications in the simulations.

*Correspondence to: Akio Ushida, Department of Electrical and Electronic Engineering, Tokushima University, Tokushima 770-8506, Japan.
†E-mail: ushida@ee.tokushima-u.ac.jp

Received 8 November 2002
Revised 17 February 2004

On the other hand, there have been published many papers concerning to the analysis of transient responses of lossy interconnects coupled with non-linear terminations. Their analytical methods are roughly classified into 3 groups. The first is the *method of characteristics* as shown in Reference [10] which is based on the reflection mechanism proposed by Branin [11]. The second is the *scattering matrix method* as shown in Reference [12, 36], etc. The third uses the *method of inverse Laplace transform* as shown in References [13–17]. They are usefully applied to the linear systems. The responses with non-linear terminations are calculated by the combination of the recursive convolution methods [14, 18, 19].

Nowadays, asymptotic waveform evaluation (AWE) [20] is widely used as a reduction technique of large-scale networks coupled with interconnects, whose algorithm is based on the moment-matching method and the Padè approximation [21, 22]. Unfortunately, one of the serious problems of the AWE is that the poles far from the origin sometimes become erroneous, because the admittance or impedance matrix in the AWE is firstly described by the power series of the complex frequency s using the Maclaurin expansion [20], and after then, it is transformed into the corresponding rational function by the application of the Padè approximation.

To overcome the problem, Nakhla *et al.* have proposed complex frequency hopping (CFH) [23] for calculating the exact poles. The algorithm can find out the exact poles by properly hopping the origin of Taylor expansion on the complex axis. The other is based on a multi-point Padè approximation [24]. Both of them need properly to choose some points in the complex frequency domain to obtain the exact Taylor series. Thus, it can find the good Padè approximation. We have also proposed an elegant method in Reference [25]. In these reduction algorithms, the reduced circuits sometimes become unstable in the time domain even if all the poles are located in the left-hand side of the complex plane. The ill-condition can be overcome by Padè via a Lanczos (PVL) process [26]. The passive reduced-order interconnect macromodelling algorithm (PRIMA) [2, 27] is an extension of the block Arnoldi technique to include the guaranteed passivity. In order to apply this algorithm to the circuits with interconnects, we need two steps such that each interconnect is modelled by a finite-order system, and Arnoldi-based congruence transform is applied to the system to form its reduced-order model [28].

On the other hand, it is said that a circuit is defined as passive if it satisfies the law of conservation of energy. Depending on the definition, it is of general perception that if the frequency response of the reduced-model is matched with the original response up to the highest frequency of interest, the passivity can be preserved [29]. Another efficient passive reduction algorithm satisfying the above passivity condition is given in Reference [30].

In this paper, we consider LSIs such that large-scale gate-array circuits are coupled with interconnects embedded in the substrate. In this case, the capacitance component of the interconnect is dominant compared to the inductance, and the diffusion resistance is very large compared to those of PCBs [3], so that we can assume them as RCG interconnects instead of RLCG. We first derive the impedance matrix at the near and far end of the interconnect [1]. All the poles of the impedance matrix are located on the negative real axis in the complex plane, and they will be easily calculated by a commercial software. Using the poles, we approximately describe each element of the matrix in a form of partial fraction, where the residues are calculated by the least squares method in such a manner that the response curves coincide with those from the impedance matrix in the complex frequency domain of interest. We found from the simulation results that the impedance matrix can be approximately

described by the partial fractions with few dominant poles located near the origin. Therefore, our reduction rate will be very large especially for large-scale interconnects. Since each element of the impedance matrix can be approximately described by a series of partial fractions, it is easily realized by the asymptotic equivalent circuit satisfying the partial fractions. Thus, we can easily develop SPICE oriented simulators of LSIs coupled with RCG interconnects. In Section 2, we show how to calculate the exact poles and residues. In Section 3, it is shown that the impedance matrix of interconnect can be well approximated with few dominant terms of the partial fractions. Thus, we can realize the simple asymptotic equivalent circuit familiar with SPICE. We can also show that the circuit is always passive. In Section 4, our reduction algorithm is shown using an example of the large-scale RCG interconnects. We found from the results that the reduction rate of our method is very large. In Section 5, some interesting examples are shown with our SPICE-oriented simulators. We found from the examples that our asymptotic equivalent method for the interconnects can get the good results even for the lower order approximation.

2. CALCULATION OF THE EXACT POLES AND RESIDUES OF INTERCONNECTS

Now, consider a uniform N coupled RCG interconnect. Let us assume the telegraph equation can be described by

$$\frac{\mathrm{d}\mathbf{V}(x,s)}{\mathrm{d}x} = -\mathbf{R}\mathbf{I}(x,s), \quad \frac{\mathrm{d}\mathbf{I}(x,s)}{\mathrm{d}x} = -(\mathbf{G}+s\mathbf{C})\mathbf{V}(x,s) \tag{1}$$

in the complex frequency domain, where $\mathbf{R}, \mathbf{C}$ and $\mathbf{G}$ are positive definite symmetric matrices.

Let us introduce matrices $\mathbf{P}_v(s)$ and $\mathbf{P}_c(s)$ to transform the circuit equations into the diagonal forms, which satisfy

$$\begin{aligned} \mathrm{diag}[\gamma_i(s)^2] &= \mathbf{P}_v(s)^{-1}\mathbf{R}(\mathbf{G}+s\mathbf{C})\mathbf{P}_v(s) \\ \mathrm{diag}[\gamma_i(s)^2] &= \mathbf{P}_c(s)^{-1}(\mathbf{G}+s\mathbf{C})\mathbf{R}\mathbf{P}_c(s) \end{aligned} \tag{2}$$

Then, the input and output relations at the near and far ends are described by the impedance matrix as follows [1, 31]:

$$\begin{bmatrix} \mathbf{V}(0,s) \\ \mathbf{V}(d,s) \end{bmatrix} = \begin{bmatrix} \mathbf{Z}_{11}(s) & \mathbf{Z}_{12}(s) \\ \mathbf{Z}_{21}(s) & \mathbf{Z}_{22}(s) \end{bmatrix} \begin{bmatrix} \mathbf{I}(0,s) \\ -\mathbf{I}(d,s) \end{bmatrix} \tag{3}$$

where

$$\begin{aligned} \mathbf{Z}_{11}(s) &= \mathbf{Z}_{22}(s) = \mathbf{P}_v(s)\mathrm{diag}[\coth\ \gamma_i(s)d]\mathbf{P}_c(s)^{-1} \\ \mathbf{Z}_{12}(s) &= \mathbf{Z}_{21}(s) = \mathbf{P}_v(s)\mathrm{diag}[\sinh\ \gamma_i(s)d]^{-1}\mathbf{P}_c(s)^{-1} \end{aligned} \tag{4}$$

Observe that all the poles of the impedance matrix are found at the locations satisfying $\sinh\ \gamma_i(s)d = 0$. Thus, we have the following theorem for the calculation of the poles.

Theorem 1
The locations of the poles satisfying relations (3) are found by solving the following equations [25]:

$$\left|\mathbf{R}(\mathbf{G}+s\mathbf{C})+\left(\frac{n\pi}{d}\right)^2\mathbf{I}\right|=0,\quad n=1,2,\ldots \tag{5}$$

where d is the length of the interconnect. For $n=0$, we have $|\mathbf{G}+s\mathbf{C}|=0$.

It can be also proved [32] that if $\mathbf{R},\mathbf{C}$ and $\mathbf{G}$ are positive definite symmetric matrices, then, all the poles of RCG interconnect are located in the negative real axis. Thus, the poles satisfying (5) can be obtained by solving the following relation:

$$|s\mathbf{I}-\mathbf{A}|=0 \quad \text{for } \mathbf{A}=-(\mathbf{RC})^{-1}\left(\left(\frac{n\pi}{d}\right)^2\mathbf{I}+\mathbf{RG}\right) \tag{6}$$

where we can efficiently use a commercial software (for example Reference [33]) to calculate the eigenvalues of $\mathbf{A}$.

To describe the impedance matrix (3) with partial fractions, we need to calculate the residues corresponding to the above poles.

Theorem 2
For the case of $n\neq 0$ in (5), the residues of $\mathbf{Z}_{12}(s)$ and $\mathbf{Z}_{21}(s)$ in (4) at the pole p_i are given by

$$\mathbf{k}_{12,i}=\mathbf{k}_{21,i}=\mathbf{P}_v(s)\text{diag}\left[0\cdots\overset{i}{\left(\frac{1}{\cosh(\gamma_i(s)d)(\partial\gamma_i(s)/\partial s)d}\right)}\cdots 0\right]\mathbf{P}_c(s)^{-1}\Big|_{s=p_i} \tag{7}$$

where $\partial\gamma_i(s)/\partial s$ is obtained as follows [20]:

$$\begin{bmatrix}\dfrac{\partial\mathbf{U}_i}{\partial s}\\ \dfrac{\partial\gamma_i(s)}{\partial s}\end{bmatrix}=\begin{bmatrix}\mathbf{R}(\mathbf{G}+s\mathbf{C})-\gamma_i(s)^2\mathbf{I} & -2\gamma_i(s)\mathbf{U}_i\\ \mathbf{U}_i^{\mathrm{T}} & 0\end{bmatrix}^{-1}\begin{bmatrix}-\mathbf{RCU}_i\\ 0\end{bmatrix} \tag{8}$$

where $\mathbf{U}_i$ is an eigenvector for $\gamma_i(s)$ given in Equation (2).

Corollary 2.1
The residues of $\mathbf{Z}_{11}(s)$ and $\mathbf{Z}_{22}(s)$ in Equation (4) are given by

$$\mathbf{k}_{12,i}=\mathbf{k}_{21,i}=\mathbf{P}_v(s)\text{diag}\left[0\cdots\overset{i}{\left(\frac{1}{(\partial\gamma_i(s)/\partial s)\,d}\right)}\cdots 0\right]\mathbf{P}_c(s)^{-1}\Big|_{s=p_i} \tag{9}$$

Observe that the residues given by Equations (7) and (9) are the same except for the signs, because the denominator of (7) has the factor $\cosh(\gamma_i(s)d)$ which takes the value '1' or '-1' depending on $\gamma_i(s)d|_{s=p_i}=jn\pi,\ i=1,2,\ldots,N,\ n=1,2,\ldots$.

Now, let us calculate the poles p_{0i} and the residues $\mathbf{k}_{011,i}=\mathbf{k}_{022,i},\ \mathbf{k}_{012,i}=\mathbf{k}_{021,i}$ at $n=0$.

Corollary 2.2
Since the poles $s = p_{0i}$ at $n = 0$ correspond to $\gamma_i \to 0$, we have the following relation:

$$\lim_{\mathbf{\Gamma}(s)\to\mathbf{0}} \mathbf{P}_v(s)\text{diag}[\sinh\ \gamma_i(s)d]^{-1}\mathbf{P}_c(s)^{-1} = (\mathbf{G} + s\mathbf{C})^{-1}/d \tag{10}$$

It can be transformed into the diagonal form [32]. Furthermore, we can show from Equation (10) that $\mathbf{k}_{012,i} = \mathbf{k}_{021,i}$ are equal to $\mathbf{k}_{011,i} = \mathbf{k}_{022,i}$.

Thus, the impedance matrix given by Equation (4) is described by the partial fractions with the poles and the corresponding residues in the following form:

$$Z_{11,ij}(s) = Z_{22,ij}(s) = \frac{k_{0,ij}}{s - p_0} + \frac{k_{1,ij}}{s - p_1} + \frac{k_{2,ij}}{s - p_2} + \frac{k_{3,ij}}{s - p_3} + \cdots \tag{11}$$

$$Z_{12,ij}(s) = Z_{21,ij}(s) = \frac{k_{0,ij}}{s - p_0} - \frac{k_{1,ij}}{s - p_1} + \frac{k_{2,ij}}{s - p_2} - \frac{k_{3,ij}}{s - p_3} + \cdots \tag{12}$$

It is very important to estimate the number of terms in Equations (11) and (12) which should be chosen to approximate the impedance matrix given by Equation (4). We consider here the special case of single line interconnect, where the input and output of an interconnect are described by the impedance matrix as follows:

$$\begin{bmatrix} V(0,s) \\ V(d,s) \end{bmatrix} = Z_0(s) \begin{bmatrix} \coth\ \gamma(s)d & (\sinh\ \gamma(s)d)^{-1} \\ (\sinh\ \gamma(s)d)^{-1} & \coth\ \gamma(s)d \end{bmatrix} \begin{bmatrix} I(0,s) \\ -I(d,s) \end{bmatrix} \tag{13}$$

$$Z_0(s) = \sqrt{R/(G + sC)}, \quad \gamma(s) = \sqrt{R(G + sC)} \tag{14}$$

We assumed the parameters as follows: $R = 5\ \Omega/\mu\text{m}$, $C = 6.28$ fF/μm, $G = 10$ mS/μm, $d = 5$ μm.

The frequency responses of $Z_{11}(s) = Z_{22}(s)$ and $Z_{12}(s) = Z_{21}(s)$ for the 20th order approximation[‡] are shown in Figure 1(a) and 1(b), respectively. We found from the example that both frequency response curves are good agreement on the whole frequency-domain. Thus, we can expect to have the good result of the transient response with the asymptotic equivalent circuit realized by relation (11) and (12), whose algorithm is shown in the next section.[§]

3. ASYMPTOTIC EQUIVALENT CIRCUIT AND ITS PASSIVITY

Now, consider the equivalent circuit for realizing the impedance matrix given by Equation (4). We have already shown in Section 2 that all the poles are located on the negative real axis. Furthermore, only the poles located near the origin will give large effect to the transient response. Therefore, we need to choose the few dominant poles around the origin. For simplicity, we consider the asymptotic equivalent circuit for the single line interconnect given

[‡]The *n*th order approximation means that we take first *n* terms of Equations (11) and (12).
[§]You can see the same result in Reference [25] for RLCG interconnect.

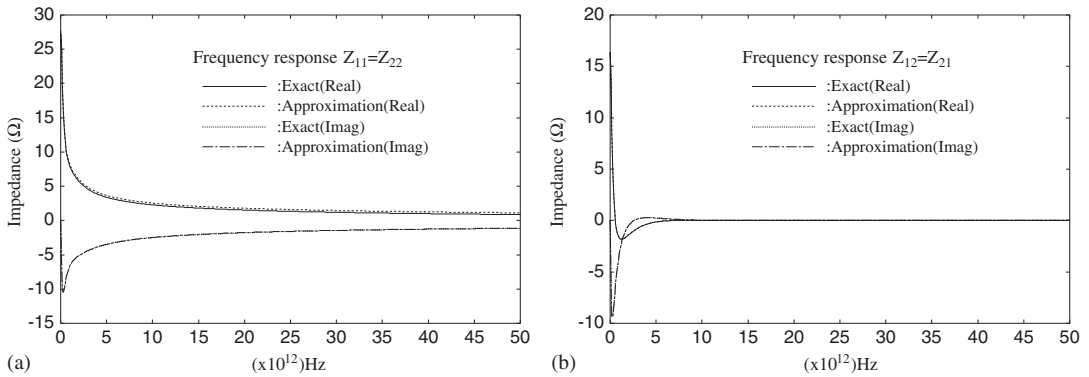

Figure 1. Approximation of partial fraction (Order = 20).

by Equations (13) and (14). Of course, the method can be easily extended to an N-coupled interconnect. We have from Equations (11) and (12) the following relations:

$$Z_{11}(s) = Z_{22}(s) = \frac{k_0}{s - p_0} + \sum_{i=1}^{M} \left[\frac{k_{2i-1}}{s - p_{2i-1}} + \frac{k_{2i}}{s - p_{2i}} \right] \tag{15}$$

$$Z_{12}(s) = Z_{21}(s) = \frac{k_0}{s - p_0} + \sum_{i=1}^{M} \left[-\frac{k_{2i-1}}{s - p_{2i-1}} + \frac{k_{2i}}{s - p_{2i}} \right] \tag{16}$$

where M is the number of dominant terms. Equations (15) and (16) consist of the same terms with the different signs. Therefore, let us set them as follows:

$$Z_1(s) = \sum_{i=0}^{M} \frac{k_{2i}}{s - p_{2i}}, \quad Z_2(s) = \sum_{i=1}^{M} \frac{k_{2i-1}}{s - p_{2i-1}} \tag{17}$$

where the poles and the residues are calculated from Equations (5), (7), (9) and (10) as follows:

$$p_0 = -\frac{G}{C}, \quad p_i = -\frac{RG + (i\pi/d)^2}{RC}, \quad i = 1, 2, \ldots, 2M \tag{18}$$

$$k_0 = \frac{1}{Cd}, \quad k_i = \frac{2}{Cd}, \quad i = 1, 2, \ldots, 2M \tag{19}$$

Then, Equations (13) and (14) can be approximately written in the following form:

$$\begin{bmatrix} V(0,s) \\ V(d,s) \end{bmatrix} = \begin{bmatrix} Z_1(s) + Z_2(s) & Z_1(s) - Z_2(s) \\ Z_1(s) - Z_2(s) & Z_1(s) + Z_2(s) \end{bmatrix} \begin{bmatrix} I(0,s) \\ -I(d,s) \end{bmatrix} \tag{20}$$

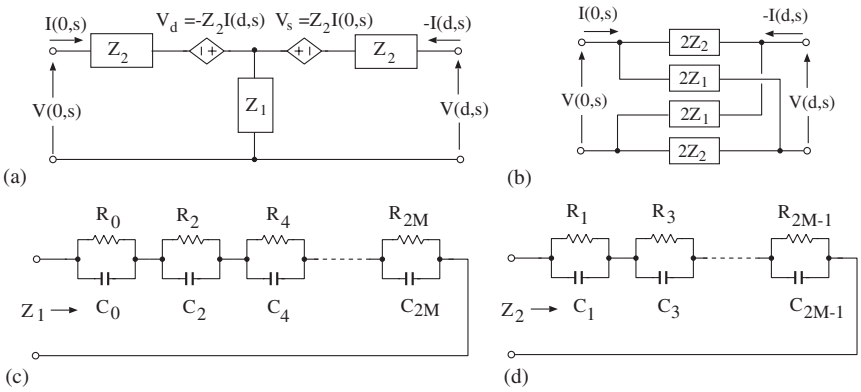

Figure 2. Asymptotic equivalent circuit.

The impedance matrix (20) contains the terms $-Z_2(s)I(d,s)$ and $Z_2(s)I(0,s)$, which can be synthesized by the use of the current-controlled voltage sources

$$V_d(s) = -Z_2(s)I(d,s), \quad V_s(s) = Z_2(s)I(0,s) \tag{21}$$

as shown in Figure 2(a). The controlled voltage sources play the important role of the reflections from both ends. We can also realize (20) by a lattice circuit as shown in Figure 2(b). The impedances Z_1 and Z_2 in Figure 2(a) and (b) are synthesized by the series connection of R–C circuits as shown in Figure 2(c) and (d), where

$$C_i = \frac{1}{k_i}, \quad R_i = -\frac{k_i}{p_i}, \quad \text{for } p_i < 0 \quad i = 0,1,2,\ldots,2M \tag{22}$$

Observe that these asymptotic equivalent circuits are very simple and familiar with SPICE. Thus, we can easily develop the user-friendly simulator. The equivalent circuits for the multiconductor interconnects can be realized in the same way as shown in the next section.

Remark that the asymptotic equivalent circuit is realized in two different ways as shown in Figure 2(a) and 2(b). Since all the resistive and capacitive elements in Z_1 and Z_2 are always positive as shown by Equation (22), the circuit (b) is passive because it does not contain any controlled source. Thus, the circuit (a) is also passive because they are equivalent in each other. Although both circuits will have the same v–i characteristics, the applications of the latter may be somewhat limited because the lower terminals are connected through $2Z_2$. See References [25, 34] for the other circuit structures of RLCG interconnects.

4. LARGE-SCALE RCG INTERCONNECTS

Let us consider the reduction algorithm of large-scale RCG interconnects and the asymptotic equivalent circuit models. To understand our algorithm, we consider an example of N coupled interconnect whose parameters [35] are given as follows:

$$[R_{i,i} = 5\,\Omega/\mu\text{m}, \quad i = 1,2,\ldots,N, \text{ Other elements of } \mathbf{R} \text{ are zeros}] \tag{23}$$

Table I. Poles for $N=1$ ($|p_{\max}|<400$).

No.	$n=0$	$n=1$	$n=2$	$n=3$	$n=4$	$n=5$
1	−1.5924	−14.165	−51.883	−114.75	−202.76	−315.92

Table II. Poles for $N=2$ ($|p_{\max}|<400$).

No.	$n=0$	$n=1$	$n=2$	$n=3$	$n=4$	$n=5$
1	−1.5544	−13.288	−48.276	−106.59	−188.23	−293.21
2	−1.6248	−15.191	−56.101	−124.28	−219.72	−342.48

Table III. Poles for $N=10$ ($|p_{\max}|<400$).

No.	$n=0$	$n=1$	$n=2$	$n=3$	$n=4$	$n=5$
1	−1.4957	−12.652	−45.693	−100.76	−177.86	−276.98
2	−1.5151	−12.795	−46.269	−102.06	−180.16	−280.58
3	−1.5419	−13.038	−47.264	−104.26	−184.08	−286.71
4	−1.5702	−13.381	−48.643	−107.41	−189.69	−295.48
5	−1.5953	−13.825	−50.456	−111.51	−196.98	−306.88
6	−1.6146	−14.356	−52.640	−116.45	−205.77	−320.62
7	−1.6275	−14.946	−55.073	−121.95	−215.58	−335.96
8	−1.6347	−15.540	−57.537	−127.53	−225.52	−352.72
9	−1.6379	−16.063	−59.707	−132.45	−234.28	−362.01
10	−1.6387	−16.426	−61.217	−135.87	−240.03	−374.76

$$\begin{bmatrix} G_{i,i}=10\ \text{mS/}\mu\text{m},\ G_{i,i-1}=G_{i,i+1}=-1\ \text{mS/}\mu\text{m}, \\ G_{i,i-2}=G_{i,i+2}=-0.1\ \text{mS/}\mu\text{m} \\ i=1,2,\ldots,N,\ \text{Other elements of } \mathbf{G} \text{ are zeros} \end{bmatrix} \tag{24}$$

$$\begin{bmatrix} C_{i,i}=6.28\ \text{fF/}\mu\text{m},\ C_{i,i-1}=C_{i,i+1}=-0.49\ \text{fF/}\mu\text{m}, \\ C_{i,i-2}=C_{i,i+2}=-0.03\ \text{fF/}\mu\text{m} \\ i=1,2,\ldots,N,\ \text{Other elements of } \mathbf{C} \text{ are zeros} \end{bmatrix} \tag{25}$$

and assume the length $d=5\ \mu$m. Using relation (5), we found the poles as shown in Tables I–III where the poles less than −400 are neglected, because they will give only small effect to the transient response, where $N=1,2,10$ means a single line, 2-coupled and 10-coupled interconnects, respectively. It is remarkable that the number of poles for N-coupled interconnect is given by $N\times(M+1)$ if we take into account until $n=0,1,\ldots,M$ in Equation (5) for

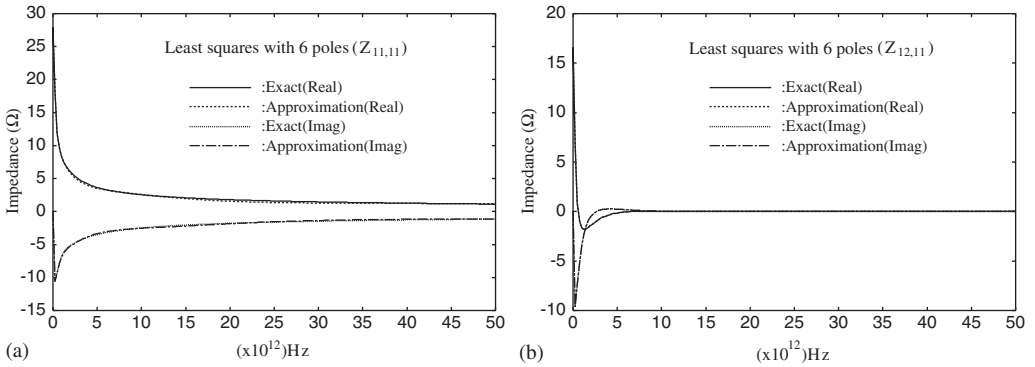

Figure 3. Least squares method with 6 poles: (a) $Z_{11,11}$; (b) $Z_{12,11}$.

the pole calculation. Thus, the number of poles rapidly increases with M and N, which causes the asymptotic equivalent circuit to complicate, especially for the large-scale interconnects.

We found from the tables that the poles for $N=1$ are always located around the central position for every nth pole groups; i.e. they are located between No.1 and No.2 for $N=2$, and between No.5 and No.6 for $N=10$ as shown in Tables II and III. Hence, in our reduction algorithm, we shall use the 6 poles for $N=1$ given in Table I, as *the dominant poles* for all the cases of N even if $N=100,1000$ or more.

In this case, each matrix element given by Equation (4) can be described by the 6 terms in the following form:

$$Z_{kl,ij}=\frac{k_{1,kl,ij}}{s+1.5924}+\frac{k_{2,kl,ij}}{s+14.165}+\frac{k_{3,kl,ij}}{s+51.883}+\frac{k_{4,kl,ij}}{s+114.75}+\frac{k_{5,kl,ij}}{s+202.76}+\frac{k_{6,kl,ij}}{s+315.92}$$

$$k,l=1,2,\quad i,j=1,2,\ldots,N \tag{26}$$

Note that we cannot any more apply the methods given by Theorem 2 and Corollary 2.1 to estimate the residues $k_{1,kl,ij},\ldots,k_{6,kl,ij}$.

Therefore, we propose here to apply *the least squares method* to estimate the approximate residues, in such a manner that the deviations between the frequency response curves from the impedance matrix given by Equation (4) and those from Equation (26) become the smallest in all the frequency domain of interest.¶ The frequency response curves using the 6 poles are shown in Figure 3(a) and 3(b). We also found from the numerical results that the residues far from the diagonal elements in $\mathbf{Z}_{ij}$, $i,j=1,2$ become smaller and smaller. Thus, it is enough to choose at most seven elements including the diagonal element in each row. Hence, each

¶In this calculation, we efficiently used a widely distributed computer software Lapack [33].

sub-matrix in Equation (4) can be written as follows:

$$\mathbf{Z}_{ij}(s) \simeq \begin{bmatrix} Z_{ij,11} & Z_{ij,12} & Z_{ij,13} & Z_{ij,14} & 0 & 0 & 0 & 0 & 0 & 0 & 0 \\ Z_{ij,21} & Z_{ij,22} & Z_{ij,23} & Z_{ij,24} & Z_{ij,25} & 0 & 0 & 0 & 0 & 0 & 0 \\ Z_{ij,31} & Z_{ij,32} & Z_{ij,33} & Z_{ij,34} & Z_{ij,35} & Z_{ij,36} & 0 & 0 & 0 & 0 & 0 \\ Z_{ij,41} & Z_{ij,42} & Z_{ij,43} & Z_{ij,44} & Z_{ij,45} & Z_{ij,46} & Z_{ij,47} & 0 & 0 & 0 & 0 \\ 0 & Z_{ij,52} & Z_{ij,53} & Z_{ij,54} & Z_{ij,55} & Z_{ij,56} & Z_{ij,57} & Z_{ij,58} & 0 & 0 & 0 \\ 0 & 0 & Z_{ij,63} & Z_{ij,64} & Z_{ij,65} & Z_{ij,66} & Z_{ij,67} & Z_{ij,68} & Z_{ij,69} & 0 & 0 \\ \cdots & \cdots & \cdots & \cdots & \cdots & \cdots & \cdots & \cdots & \cdots & \cdots & \cdots \\ 0 & 0 & 0 & 0 & 0 & 0 & 0 & Z_{ij,NN-3} & Z_{ij,NN-2} & Z_{ij,NN-1} & Z_{ij,NN} \end{bmatrix} \tag{27}$$

for $i, j = 1, 2$. We also found from the results that the diagonal terms in $\mathbf{Z}_{11}(s) = \mathbf{Z}_{22}(s)$ and $\mathbf{Z}_{12}(s) = \mathbf{Z}_{21}(s)$ are most dominant. Furthermore, we have the following relations:

$$\begin{bmatrix} Z_{ij,11} \approx \cdots \approx Z_{ij,NN}, \text{ for diagonal elements} \\ Z_{ij,kk+1} \approx Z_{ij,kk-1}, Z_{ij,kk+2} \approx Z_{ij,kk-2}, Z_{ij,kk+3} \approx Z_{ij,kk-3}, \text{ for nonzero } k\text{th terms} \end{bmatrix} \tag{28}$$

Using relations (3) and (28), the terminal voltages at the near and far ends can be written as follows:

$$\begin{aligned} V_k(0,s) \approx\ & Z_{11,kk} I_k(0,s) + Z_{11,kk+1}(I_{k-1}(0,s) + I_{k+1}(0,s)) \\ & + Z_{11,kk+2}(I_{k-2}(0,s) + I_{k+2}(0,s)) + Z_{11,kk+3}(I_{k-3}(0,s) + I_{k+3}(0,s)) \\ & + Z_{12,kk} I_k(d,s) + Z_{12,kk+1}(I_{k-1}(d,s) + I_{k+1}(d,s)) \\ & + Z_{12,kk+2}(I_{k-2}(d,s) + I_{k+2}(d,s)) + Z_{12,kk+3}(I_{k-3}(d,s) + I_{k+3}(d,s)) \end{aligned} \tag{29}$$

$$\begin{aligned} V_k(d,s) \approx\ & Z_{12,kk} I_k(0,s) + Z_{12,kk+1}(I_{k-1}(0,s) + I_{k+1}(0,s)) \\ & + Z_{12,kk+2}(I_{k-2}(0,s) + I_{k+2}(0,s)) + Z_{12,kk+3}(I_{k-3}(0,s) + I_{k+3}(0,s)) \\ & + Z_{11,kk} I_k(d,s) + Z_{11,kk+1}(I_{k-1}(d,s) + I_{k+1}(d,s)) \\ & + Z_{11,kk+2}(I_{k-2}(d,s) + I_{k+2}(d,s)) + Z_{11,kk+3}(I_{k-3}(d,s) + I_{k+3}(d,s)) \\ & k = 1, 2, \ldots, N \end{aligned} \tag{30}$$

$Z_{11,kk}$ in the first term of Equation (29) and the fifth term of Equation (30) correspond to the self-impedances $Z_{11}, Z_{22}, \ldots, Z_{NN}$ as shown in Figures 4(b) and 5(b). Other terms consist of the current-controlled voltage sources as shown Figure 5(a).

We found from the example that the reduction rate is very large, because the impedance matrix can be approximated with few dominant elements around the diagonals as shown in Equation (27). If the coupling coefficients between the multi-conductors ((23)–(25)) become stronger, we may take into account some more off-diagonal elements of $\mathbf{Z}_{ij}(s)$, $i, j = 1, 2$.

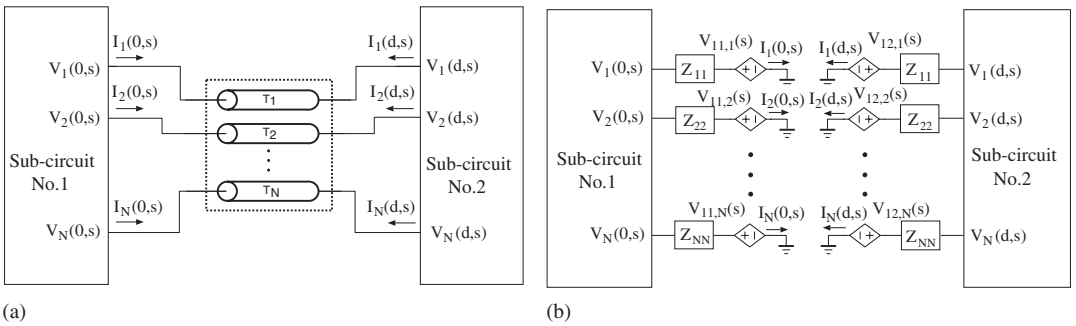

Figure 4. (a) Multi-conductor interconnect coupled with LSIs; and (b) SPICE model of the multi-conductor interconnect.

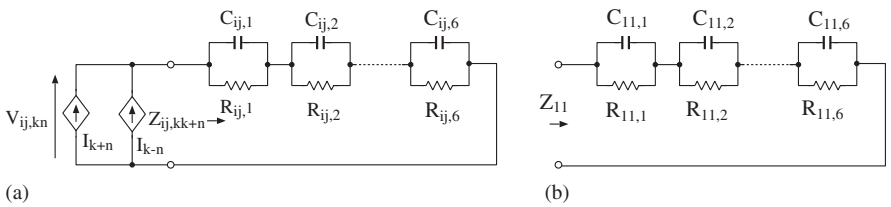

Figure 5. (a) Current-controlled voltage source; and (b) self-impedance.

5. ILLUSTRATIVE EXAMPLES

5.1. Crosstalk

In order to investigate the crosstalks, we consider a 4 coupled interconnect as shown in Figure 6(a), whose parameters are given by Equations (23)–(25). The transient responses at near and far ends of 4 coupled lines are shown in Figure 6. They have relatively large crosstalk.

5.2. Inverter circuit

Now, we consider inverter circuit coupled by interconnects as shown in Figure 7(a). Let us assume the parameters as follows [3]:

$$[R_{i,i} = 50\,\Omega/\mu\text{m},\ i = 1, 2, \ldots, N,\ \text{Other elements of } \mathbf{R} \text{ are zeros}]$$

$$\left[\begin{array}{l} G_{i,i} = 0.01\ \text{mS}/\mu\text{m}, G_{i,i-1} = G_{i,i+1} = -0.002\ \text{mS}/\mu\text{m}, \\ G_{i,i-2} = G_{i,i+2} = -0.0004\ \text{mS}/\mu\text{m} \\ i = 1, 2, \ldots, N,\ \text{Other elements of } \mathbf{G} \text{ are zeros} \end{array}\right]$$

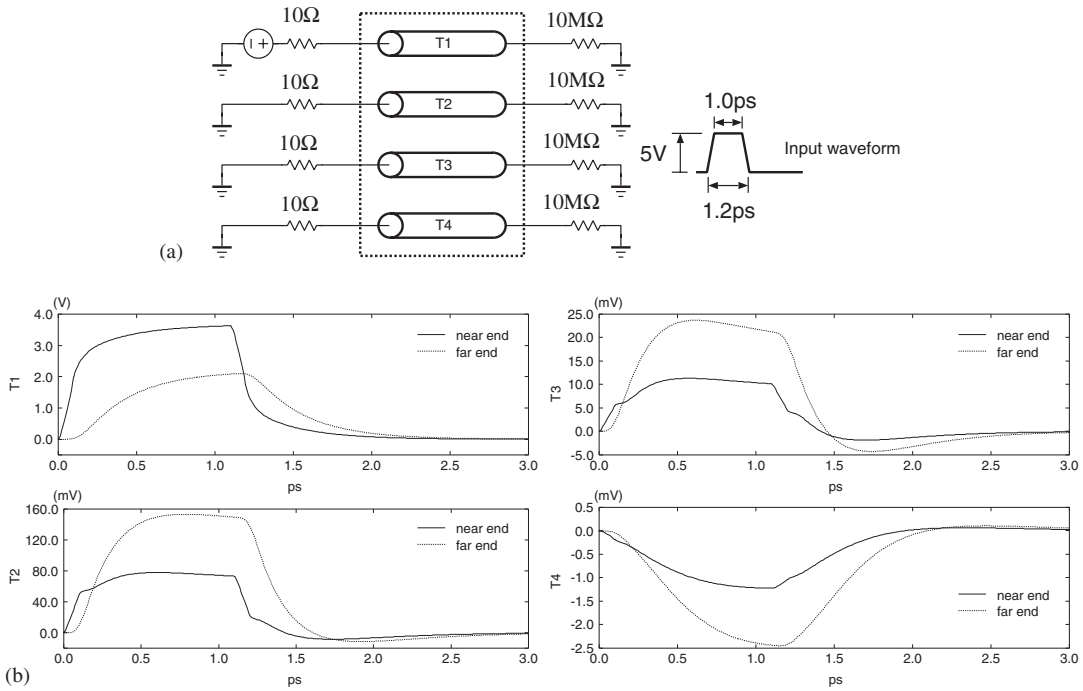

Figure 6. (a) 4-coupled interconnects; and (b) crosstalks.

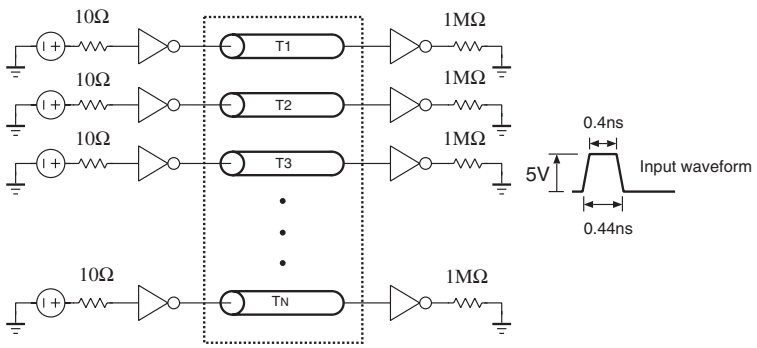

Figure 7. Inverter circuit, $d = 20\ \mu\text{m}$.

$$\begin{bmatrix} C_{i,i} = 1.0\ \text{fF}/\mu\text{m}, C_{i,i-1} = C_{i,i+1} = -0.2\ \text{fF}/\mu\text{m}, \\ C_{i,i-2} = C_{i,i+2} = -0.04\ \text{fF}/\mu\text{m} \\ i = 1, 2, \ldots, N, \text{ Other elements of } \mathbf{C} \text{ are zeros} \end{bmatrix}$$

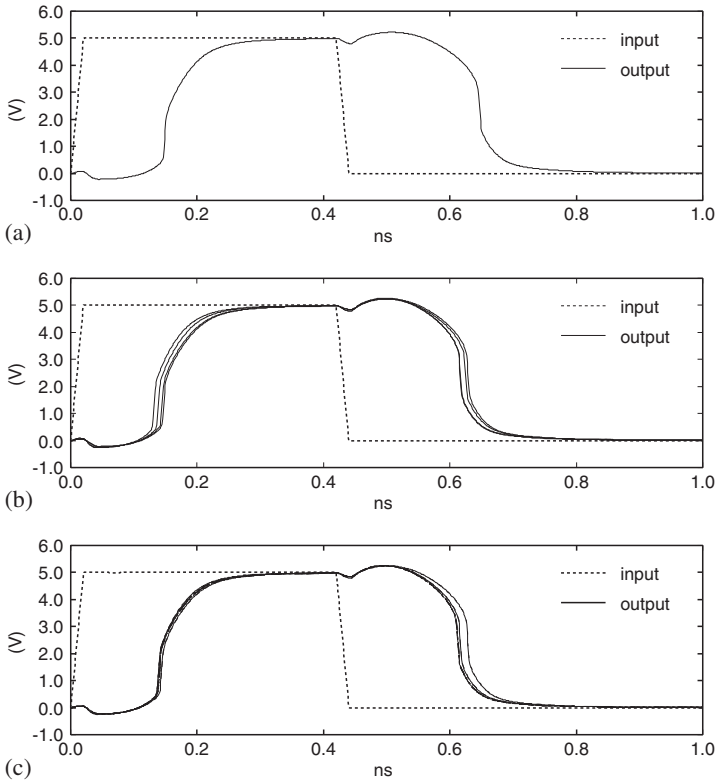

Figure 8. Transient responses: (a) $N = 1$; (b) $N = 4$; and (c) $N = 10$.

We always used the 6 poles from $N = 1$ as the *dominant poles* for the coupled interconnect, and the residues are estimated by the least squares method as shown in Section 4. The responses for $N = 1$, 4 and 10 are shown in Figure 8(a), (b) and (c), respectively. Observe that the response of the central line of the interconnect has the largest time-delay. Their phenomena are caused by both interconnects and inverters.

5.3. A fulladder circuit coupled with interconnects

Consider a fulladder circuit coupled with interconnects as shown in Figure 9(a). The coupling parameters are the same as those of the inverter circuit in example 5.2. The transient responses at the output stages are shown by solid lines in Figure 9(b), where the dotted lines show the responses without the interconnects. Observe that the responses with the coupled interconnects show complicated phenomena combining the time-delays, crosstalks, reflections, etc.

6. CONCLUSIONS AND REMARKS

In this paper, we have proposed a reduction algorithm for large-scale RCG interconnects, where the interconnects are replaced by simple asymptotic equivalent circuits familiar with

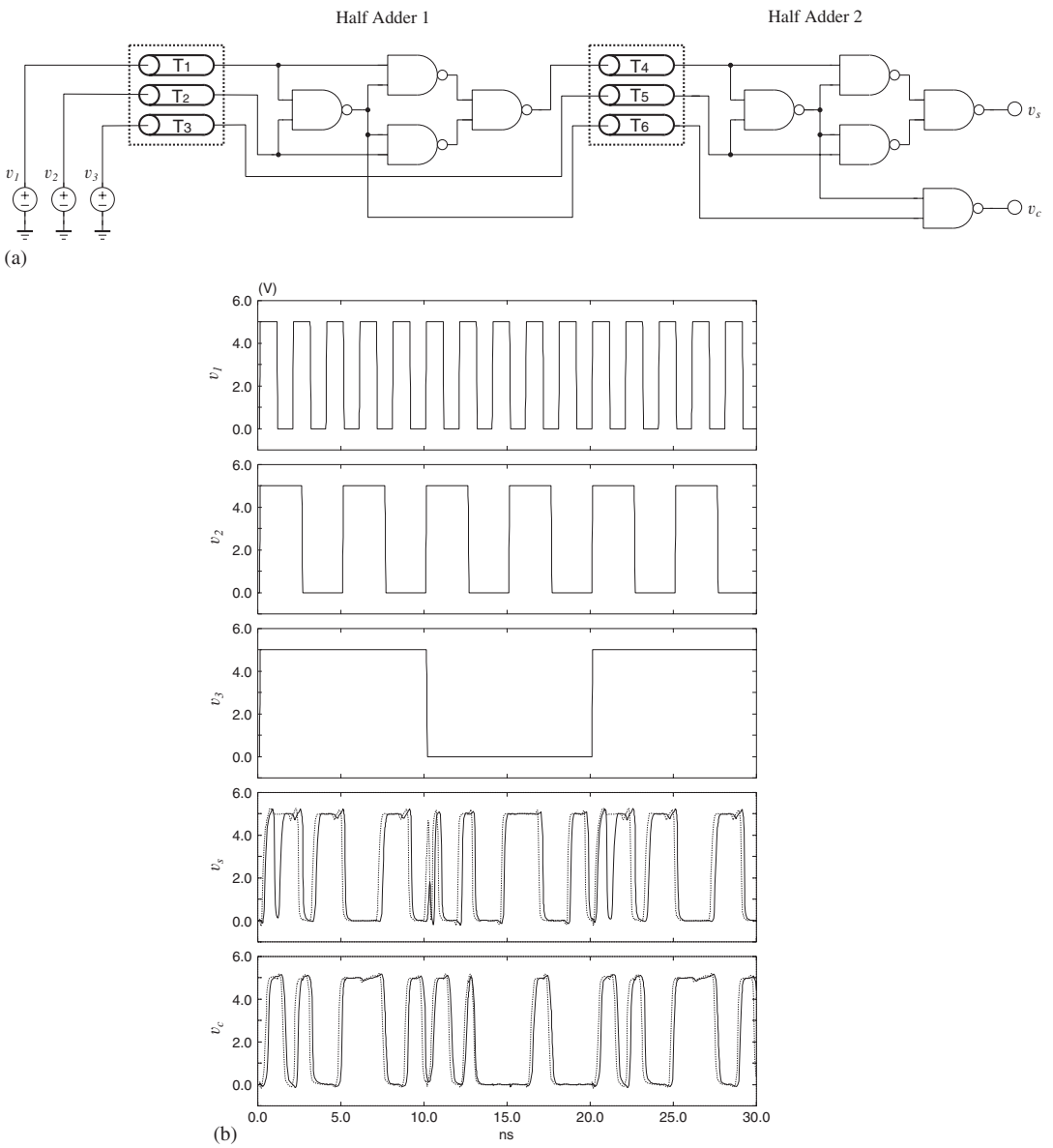

Figure 9. (a) Fulladder coupled with interconnects $d = 20\,\mu\text{m}$; and (b) transient response of the fulladder circuit, v_1, v_2, v_3: inputs, v_s, v_c: outputs. The solid lines show the responses with coupled interconnects, and the dotted lines show the responses without the interconnects.

SPICE. The algorithm will be efficiently applied to such a large-scale circuit coupled with interconnects in the substrate.

In Section 2, we showed that a numerical algorithm for computing the exact poles and the residues given by the impedance matrix. Thus, the impedance matrix is described in the form

of partial fractions. The partial fractions are realized by the asymptotic equivalent circuits as shown in Section 3. In Section 4, we have applied it to large-scale interconnects, where the residues are estimated by the least squares method instead of the analytical method. We found from the numerical examples that the impedance matrices are approximated by very simple sparse matrices, whose dominant elements are distributed around the diagonal elements. Thus, the reduction rate is very large especially for large-scale interconnects.

For the future work, we want to extend the algorithm to the large-scale RLCG interconnects.

ACKNOWLEDGEMENTS

The authors would like to thank a manager of Sony Co. Mr K. Ogawa for giving us important suggestions, and ME student of Tokushima University Mr H. Sakaguchi for his help to the numerical experiments.

REFERENCES

1. Brandao Faria JA. *Multiconductor Transmission-Line Structures: Modal Analysis Techniques*. Wiley: New York, 1993.
2. Celik M, Pileggi L, Odabasioglu A. *IC Interconnect Analysis*. Kluwer Academic Publishers: Dordrecht, 2002.
3. Wyatt Jr JL. Signal propagation delay in RC models for interconnect. In *Circuit Analysis, Simulation and Design*, Ruehli AE (ed.). Elsevier, North-Holland: Amsterdam, 1987; 254–291.
4. Elmore WC. The transient response of damped linear networks with particular regard to wideband amplifiers. *Journal of Applied Physics* 1948; **19**:55–63.
5. Sakurai T. Closed-form expressions for interconnection delay, coupling, and crosstalk in VLSI's. *IEEE Transactions on Electron Devices* 1991; **40**:118–124.
6. Kim S-Y, Gopal N, Pillage LT. Time-domain macromodels for VLSI interconnect analysis. *IEEE Transactions on Computer-Aided Design* 1994; **13**:1257–1270.
7. Gupta R, Tutuianu B, Pileggi LT. The Elmore delay as a bound for RC trees with generalized input signals. *IEEE Transactions on Computer-Aided Design* 1997; **16**:95–104.
8. Alpert CJ, Devgan A, Kashap CV. RC delay metrics for performance optimization. *IEEE Transactions on Computer-Aided Design* 2001; **20**:571–582.
9. Kimura T, Okumura M. An efficient reduction method of a substrate RC network model. *IEICE Transactions on Fundamentals* 2001; **E84-A**:698–704.
10. Chang FY. Waveform relaxation analysis of RLCG transmission lines. *IEEE Transactions on Circuits and Systems* 1990; **37**:1394–1415.
11. Branin FH Jr. Transient analysis of lossless transmission line. *Proceedings of IEEE* 1967; **55**:2012–2013.
12. Dhaene T, Martens L, Zutter DD. Transient simulation of arbitrary nonuniform interconnection structures characterized by scattering parameters. *IEEE Transactions on Circuits and Systems* 1992; **39**:928–937.
13. Chang EC, Kang SM. Computationally efficient simulation of a lossy transmission line with skin effect by using numerical inversion of Laplace transform. *IEEE Transactions on Circuits and Systems* 1992; **39**:861–868.
14. Roychowdhury JS, Newton AR, Pederson DO. Algorithms for the transient simulation of lossy interconnects. *IEEE Transactions on Computer-Aided Design* 1994; **13**:96–104.
15. Hosono T. *High Speed Laplace Transformation with BASIC.* Kyouritsu: Japan, 1984 (Japanese).
16. Manney SL, Nakhla MS, Zhang Q-J. Analysis of nonuniform, frequency-dependent high-speed interconnects using numerical inversion of Laplace transform. *IEEE Transactions on Computer-Aided Design* 1994; **13**: 1513–1525.
17. Ichikawa S. Numerical analysis of traveling waves in transmission networks by numerical inversion of Laplace transform. *IEE of Japan* 1982; **102**(12):785–792 (Japanese).
18. Lin S, Kuh ES. Transient simulation of lossy interconnects based on the recursive convolution formulation. *IEEE Transactions on Circuits and Systems-I* 1992; **39**:879–892.
19. Lawrence YL, Pileggi T, Strojwas AJ. ftd:Frequency to time domain conversion for reduced-order interconnect simulation. *IEEE Transactions on Circuits and Systems-I* 2001; **48**:500–506.
20. Chiprout E, Nakhla MS. *Asymptotic Waveform Evaluation and Moment Matching for Interconnect Analysis.* Kluwer Academic Publishers: Dordrecht, 1994.
21. Pillage LT, Rohrer RA. Asymptotic waveform evaluation for timing analysis. *IEEE Transactions on Computer-Aided Design* 1990; **9**:352–355.

22. Lee JY, Huang X, Rohrer RA. Pole and zero sensitivity calculation in asymptotic waveform evaluation. *IEEE Transactions on Computer-Aided Design* 1992; **11**:586–597.
23. Chiprout E, Nakhla MS. Analysis of interconnect networks using complex frequency hopping(CHF). *IEEE Transactions on Computer-Aided Design* 1995; **14**:186–200.
24. Celik M, Ocali O, Tan MA, Atalar A. Pole-zero computation in microwave circuits using multipoint Padè approximation. *IEEE Transactions on Circuits and Systems* 1995; **42**:6–13.
25. Ushida A, Urabe K, Yamagami Y, Nishio Y. Asymptotic equivalent circuits of interconnects based on complex frequency method. *ECCTD'01* 2001; **3**:29–32.
26. Feldmann P, Freund RW. Efficient linear analysis by Padè approximation via the Lanczos process. *IEEE Transactions on Computer-Aided Design* 1995; **14**:639–649.
27. Odabasioglu A, Celik M, Pileggi LT. PRIMA: passive reduced-order interconnect macromodeling algorithm. *IEEE Transactions on Computer-Aided Design* 1998; **17**:645–654.
28. Yu Q, Meiling J, Kuh ES. Passive multipoint moment matching model order reduction algorithm on multiport distributed interconnect networks. *IEEE Transactions on Circuits and Systems-I* 1999; **46**:140–160.
29. Winklestein D, Steer BB, Pomerleau R. Simulation of arbitrary transmission line networks with nonlinear terminations. *IEEE Transactions on Circuits and Systems-I* 1991; **38**:418–422.
30. Achar R, Gunupudi PK, Nakhla MS, Chiprout E. Passive interconnect reduction algorithm for distributed/measured networks. *IEEE Transactions on Circuits and Systems-II* 2000; **47**:287–301.
31. Tanji Y, Jiang L, Ushida A. Analysis of pulse response of multi-conductor transmission lines by a partitioning technique. *IEICE Transactions on Fundamentals* 1994; **E77-A**(12):2017–2027.
32. Chirlian PM. *Integrated and Active Network Analysis and Synthesis*. Prentice-Hall: Englewood Cliffs, NJ, 1967.
33. http://www.netlib.org/lapack.
34. Dhaene T, Zutter DD. Selection of lumped element models for coupled lossy transmission lines. *IEEE Transactions on Computer-Aided Design* 1992; **11**:805–815.
35. Weeks WT, Wu LL, McAllister MF, Singh A. Resistive and inductive skin effect in rectangular conductors. *IBM Journal on Research and Development* 1979; **23**(6):652–660.
36. Corey SD, Yang AT. Interconnect characterization using time-domain reflectometry. *IEEE Transactions on Microwave Theory and Techniques* 1995; **43**(9):2151–2156.

